

RESEARCH ARTICLE

Precise Trajectory Tracking of Multi-Rotor UAVs Using Wind Disturbance Rejection Approach

SHEIKH IZZAL AZID^{1,2}, (Member, IEEE),
SOHAIL AHMAD ALI¹, (Graduate Student Member, IEEE), **MESHACH KUMAR**²,
MAURIZIO CIRRINCIONE^{2,3}, (Senior Member, IEEE),
AND ADRIANO FAGIOLINI⁴, (Member, IEEE)

¹North Australia Centre for Autonomous Systems, Charles Darwin University, Darwin, NT 0810, Australia

²School of Information Technology, Engineering, Mathematics and Physics, The University of the South Pacific, Suva, Fiji

³Control Systems, University of Technology of Belfort-Montbéliard, 90016 Belfort, France

⁴Mobile and Intelligent Robots@Panormous Laboratory (MIRPALab), Department of Engineering, University of Palermo, 90128 Palermo, Italy

Corresponding author: Adriano Fagiolini (adriano.fagiolini@unipa.it)

This work was supported by The University of the South Pacific and the University of Palermo.

ABSTRACT This paper discusses the resilience of the UAV quadrotor to wind disturbances. An unknown input-state observer is presented that uses the Lipschitz method to estimate the internal states and disturbances of the quadrotor and compensate for them by varying the velocities of the four rotors. The observer intends to use existing sensor measurements to estimate the unknown states of the quadrotor and reconstruct the three-dimensional wind disturbances. The estimated states and external disturbances are sent to the PD controller, which compensates for the disturbances to achieve the desired position and attitude, as well as robustness and accuracy. The Lipschitz observer was designed using the LMI approach, and the results were validated using Matlab/Simulink and using the Parrot Mambo mini quadrotor.

INDEX TERMS Disturbance rejection, Lipschitz observer, quadrotor, trajectory.

I. INTRODUCTION

Unmanned Aerial Vehicles (UAV) have seen tremendous growth and development in recent years, largely due to advances in control systems and the miniaturization of instruments. These versatile devices have a wide range of applications, including land surveying, weather monitoring, disaster response, and surveillance. Their ability to perform tasks remotely and efficiently makes them a valuable resource in many industries and fields [1].

Despite significant advances in quadrotor control systems, an ongoing challenge is to maintain robust control in the presence of external disturbances such as wind gusts. These gusts can cause significant deviations from the intended flight path, making it difficult to achieve accurate tracking and maintain robust performance [2], [3]. These disturbances can come from a variety of sources and can be difficult to

predict or mitigate, making their effect on quadrotor flight a significant challenge to overcome.

To achieve accurate trajectory tracking and stability, it is necessary to have access to all states of the quadrotor. However, even with this information, classical control strategies may not be sufficient to effectively handle external disturbances such as wind gusts. In such cases, it is necessary to measure and compensate for these disturbances to maintain the stability and robustness of the quadrotor [4], [5].

Although it is possible to mitigate the influence of measurable disturbances using a feed-forward strategy [6], disturbances often cannot be measured directly or are too expensive to measure. Wind sensors, such as anemometers and pitot probes, used to measure wind disturbances face several challenges. First, these sensors are often bulky and heavy, which can be a problem in terms of payload and space. Second, pitot tubes, which are typically small and lightweight, may not provide accurate measurements when the UAVs fly at low speeds [7]. Finally, downwash caused by rotors can significantly affect the accuracy of wind sensor

The associate editor coordinating the review of this manuscript and approving it for publication was Jinquan Xu¹.

data, making it difficult to obtain reliable results with this direct measurement approach.

There are two ways to compensate for the disturbances, first is to design complex controllers with accurate models so that the disturbances can be compensated. Reference [8] proposed PID and intelligent active force control to enhance disturbance rejection capability and robust trajectory. Alternatively, [9] and [10] proposed backstepping and sliding mode control in a double loop structure for effective trajectory tracking for the desired position of a quadrotor model subject to disturbances. The work cited in [11] proposes high-order sliding mode control to suppress chattering compared to conventional methods while maintaining robustness, while [12] proposed adaptive sliding mode robust control of the quadrotor by bounding position error using Lyapunov theory. Adaptive integral sliding mode was also proposed to robustly control the quadrotor in presence of disturbance [13]. Fractional controllers also show good results in eliminating disturbances. Reference [14] used the lab helicopter to test the performance of robust position control under aggressive manoeuvres in presence of time varying wind. Reference [10] tested PID and LQR methods in presence of wind using wind gust model. [15], however the complexity of the controller is significant. In general, these methods aim to retain model uncertainty and external disturbance insensitivity in a variety of ways but do not estimate the disturbances to compensate. Consequently, they may be slow to respond to sudden external disturbances. Moreover tilt-rotor quadrotor is also proposed for disturbance rejection during flight with expense of additional motors [16].

Intuitively, the second solution when compared to the discussion above is to estimate the disturbance or its influence using available measurements, and then use this estimate to implement a control action that compensates for the disturbance's effects [4]. Robust observer algorithms have been developed in recent decades to address the issue of maintaining system stability and performance in the presence of external disturbances. These algorithms, including the Extended Kalman Filters (EKF), Equivalent Input Disturbance (EID) estimator, Uncertainty and Disturbance Estimator (UDE), Generalized Proportional Integral Observer (GPIO), Extended State Observer (ESO), and Extended High Gain Observer (EHGO), as well as Unknown Input Observers (UIO), allow for the estimation of both known and unknown inputs in linear and nonlinear systems [17]. The ESO and GESO methods achieve this by augmenting the state vector with estimates of the unknown inputs, which are then used to reconstruct the disturbance signals [18]. In ESO/GESO, the error between the actual and estimated output, known as the output error, is influenced by the derivative of the disturbance. When the disturbance is slowly changing, the accuracy of the estimation will be higher and the output error will converge to a small, predetermined bound determined by the observer gains. If the disturbance is constant, the output error will converge to zero asymptotically [18]. However,

wind disturbances are highly variable and tend to change quickly, making it difficult for the ESO/GESO method to accurately estimate and compensate for them. On the other hand, the Kalman filter (KF) can handle nonlinear systems by linearizing the system dynamics at each time step, making it a versatile option for highly nonlinear systems, such as the quadrotor. However, the KF method is vulnerable to any system malfunctions. If the actual condition of the system does not match the models used in the filter's design, then these discrepancies resulting from sensor or actuator failures can significantly decrease the accuracy of the estimation system [19]. Additionally, the KF requires careful manual tuning of process noise parameters and can be computationally demanding, which may be an issue for real-time applications [20]. Reference [21] proposed on improving the performance of the of Dynamic system in presence of disturbances using a new observer with input nonlinearities.

With respect to the application of the vehicles multiple complex observers has been designed for precise positioning. A frequency domain DO is developed to estimate wind disturbance in [22] In contrast, only the linearized model is considered, which cannot account for every quadrotor operation state. Reference [23] estimated the wind gusts affecting the quadrotors (a type of UAV) as the input disturbances by using a frequency-based nonlinear disturbance observer (NDOB) which is fuzzy-based. Looking at intended precise positioning, multiple complex observers have been developed for precise [24]. State prediction with input delay and external disturbance was proposed by [25], this technique was tested on the nonlinear quadrotor model. A frequency domain is developed to estimate wind disturbance by [22]. In contrast, here only the linearized model is considered, which cannot account for every quadrotor operation state. Reference [26] used Kalman filter to estimate wind gusts and [27] used the extended Kalman filter is used to estimate wind disturbance based on ESC motor command feedback however it requires numerous assumptions for noise to tune process noise and measurement noise. Drag utilization method was proposed by [28] for trajectory tracking of the quadrotor by using the wind speed observer. Linear unknown input observer also shows good results however the modeling of the quadrotor is linear [4]. Reference [23] estimated the wind gusts affecting the quadrotors as the input disturbances by using a frequency-based nonlinear disturbance observer (NDOB) which is fuzzy-based. Overall, simulations and experiments demonstrate that the observer to estimate disturbances in conjunction with simple controllers yields very good results

The paper presents a wind disturbance rejection approach, where wind disturbance is promptly estimated online by a low-computation observer. Attractive features of the developed scheme are its simplicity, low computation cost, and ability to obtain a fast response to wind gusts. It should be noted that traditional robust control involves complex controllers and is unable to react fast enough in the presence

of strong disturbances [29], [30] or requires the application of additional sensors or signals that can be too conservative. Conversely, the present approach compensates for the exact amount of disturbance that is acting on the system by a prompt online estimation, including also model uncertainties such as imprecise knowledge of the system parameters. The estimation is achieved through a low computation process whose design requires no additional sensors and which robustly estimates the overall effects of wind disturbance and other model uncertainty. It is worth noticing that the promptness and effectiveness of the proposed estimator, along with the position recovery scheme, are shown to outperform existing solutions based on EKF.

Furthermore, and yet very importantly, the proposed approach can be easily integrated into existing schemes developed by drone companies, most of which use the EKF or KF included in ArduPilot. Indeed, being independent of the type of control law used to determine the aircraft rotor speeds, the developed scheme can provide existing controllers with the additional capability to better handle disturbances; this allows its implementation on almost any aircraft system, including fixed wings, as a stand-alone solution or as an extension plugin for existing controllers and can be incorporated into ArduPilot or Mission Planners, which are mainly used for UAV missions in the UAV industry. This fact is demonstrated in the paper, both in simulation and through experiments, on a platform using an indoor programmable quadrotor.

Finally, the proposed Lipschitz observer outperforms existing solutions based on EKF and nonlinear observers with unknown input (NUIO). Indeed, it combines the advantages of NUIO approaches, in that it does not require the addition of additional state variables and modeling of their dynamics, as well as the accuracy of the estimation obtained via the model's Lipschitz property.

II. QUADROTOR MATHEMATICAL MODELING WITH DISTURBANCES

The position (x, y, z) of an aircraft's center of mass is measured by GPS sensors, which provide data in the inertial Earth frame F_0 , while the orientation (ϕ, θ, ψ) is measured by Inertial Measurement Units (IMU) in a body frame F_B . The state vector of a quadrotor vehicle consists of $(x, y, z, \phi, \theta, \psi)$ and (u, v, w, p, q, r) variables representing the vehicle's position and velocity respectively. As shown in Fig. 1, the four rotors apply a force orthogonal to the rotation plane of their blades which are aligned with the positive z -axis of the body frame F_B and proportional to the rotation speed square, i.e. $F_i = K_F \omega_i^2$, where i is the i -th rotor. Each force F_i generates a torque along the z -axis which is represented by the opposite arm of the aircraft chassis, being $lK_F \omega_i^2$, where l is the arm length. Each rotor produces a torque, due to air drag, that is opposite to its rotation and whose absolute value is proportional to its rotation speed, that is, $K_M \omega_i^2$. Therefore, the overall thrust F_z and the components of the torque vector $(\tau_\phi, \tau_\theta, \tau_\psi)$ are linearly coupled with the squares of rotor

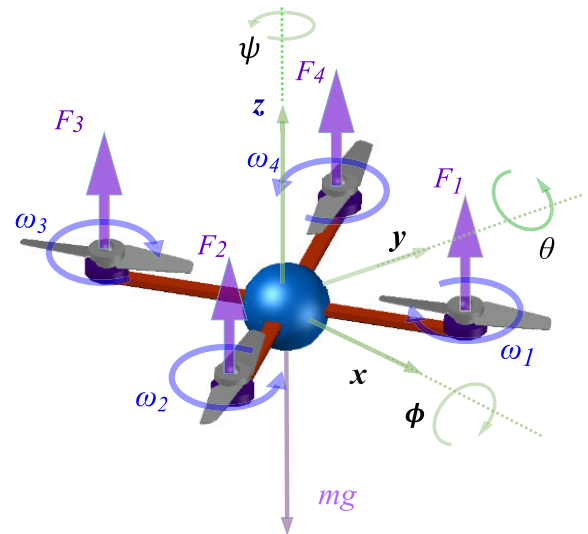


FIGURE 1. Quadrotor mechanical structure, model and reference frames.

speeds. All such quantities are grouped in the state and input vectors:

$$\xi = (x, y, z, \phi, \theta, \psi, u, v, w, p, q, r)^T, \quad (1)$$

$$U = \begin{pmatrix} F_z \\ \tau_\phi \\ \tau_\theta \\ \tau_\psi \end{pmatrix} = \begin{pmatrix} K_F(\omega_1^2 + \omega_2^2 + \omega_3^2 + \omega_4^2) \\ lK_F(\omega_2^2 - \omega_4^2) \\ lK_F(\omega_1^2 - \omega_3^2) \\ K_M(\omega_1^2 - \omega_2^2 + \omega_3^2 - \omega_4^2) \end{pmatrix}. \quad (2)$$

In addition, the ZXY convention is utilized to align the axes of F_0 and F_B . The orientation of the aircraft is determined by first rotating F_0 about the z -axis of ψ (yaw) radians, then about the x -axis of ϕ (roll) radians, and finally about the y -axis of θ (pitch) radians. Consequently, considering the fundamental rotations

$$R_x(\phi) = \begin{pmatrix} 1 & 0 & 0 \\ 0 & c_\phi & s_\phi \\ 0 & -s_\phi & c_\phi \end{pmatrix}, \quad R_y(\theta) = \begin{pmatrix} c_\theta & 0 & -s_\theta \\ 0 & 1 & 0 \\ s_\theta & 0 & c_\theta \end{pmatrix}, \quad (3)$$

$$R_z(\psi) = \begin{pmatrix} c_\psi & s_\psi & 0 \\ -s_\psi & c_\psi & 0 \\ 0 & 0 & 1 \end{pmatrix},$$

where $s_* = \sin(*)$ and $c_* = \cos(*)$, the complete rotation converting body-frame coordinates into inertial ones is

$$R_{zxy} = (R_z(\psi)R_x(\phi)R_y(\theta))^T = \begin{pmatrix} c_\theta c_\psi - s_\phi s_\theta s_\psi & -c_\phi s_\psi & s_\theta c_\psi + s_\phi c_\theta s_\psi \\ c_\theta s_\psi + s_\phi s_\theta c_\psi & c_\phi c_\psi & s_\theta s_\psi - s_\phi c_\theta c_\psi \\ -c_\phi s_\theta & s_\theta & c_\phi c_\theta \end{pmatrix}. \quad (4)$$

The forces acting on the quadrotor center of mass are the total thrust F applied by the four rotors (always aligned with the positive z -axis of the F_B), the gravity force (which is oriented along the negative direction of the z -axis of F_0), and the wind gusts, $W = (W_x, W_y, W_z)^T$ (whose components are expressed in F_0 by convention). Newton's Equation for the

translational motion of the center of mass states:

$$m \begin{pmatrix} \ddot{x} \\ \ddot{y} \\ \ddot{z} \end{pmatrix} = -m \begin{pmatrix} 0 \\ 0 \\ g \end{pmatrix} + R_{zxy} \begin{pmatrix} 0 \\ 0 \\ F \end{pmatrix} + W, \quad (5)$$

which can be expanded as

$$\begin{pmatrix} m\ddot{x} \\ m\ddot{y} \\ m\ddot{z} \end{pmatrix} = \begin{pmatrix} (s_\theta c_\psi + s_\phi c_\theta s_\psi)F + W_x \\ (s_\theta s_\psi - s_\phi c_\theta c_\psi)F + W_y \\ (c_\phi c_\theta)F - mg + W_z \end{pmatrix}, \quad (6)$$

where m is the aircraft's mass and g the gravity acceleration.

In addition, the angular velocity vector $(p, q, r)^\top$ of the aircraft in body frame F_B can be related to the Euler angles via a dynamic relation that, for the ZXY convention, reads as follows:

$$\begin{pmatrix} p \\ q \\ r \end{pmatrix} = \begin{pmatrix} 0 \\ \dot{\theta} \\ 0 \end{pmatrix} + R_y(\theta) \begin{pmatrix} \dot{\phi} \\ 0 \\ 0 \end{pmatrix} + R_y(\theta)R_x(\phi) \begin{pmatrix} 0 \\ 0 \\ \dot{\psi} \end{pmatrix},$$

which can be compactly written as

$$\begin{pmatrix} p \\ q \\ r \end{pmatrix} = \begin{pmatrix} c_\theta & 0 & -s_\theta \\ 0 & 1 & 0 \\ s_\theta & 0 & c_\theta c_\phi \end{pmatrix} \begin{pmatrix} \dot{\phi} \\ \dot{\theta} \\ \dot{\psi} \end{pmatrix}. \quad (7)$$

Due to the lean and trim structure of the quadrotor, it is assumed that the wind momentum is negligible, which implies that the vector $T = (\tau_\phi, \tau_\theta, \tau_\psi)^\top$ acting on the aircraft itself is composed of the rotor torques. Since F_B is aligned with the aircraft's principal inertia axes, Euler's equations for the angular motion are as follows:

$$T = I \begin{pmatrix} \dot{p} \\ \dot{q} \\ \dot{r} \end{pmatrix} + \begin{pmatrix} 0 & -r & q \\ r & 0 & -p \\ -q & p & 0 \end{pmatrix} I \begin{pmatrix} p \\ q \\ r \end{pmatrix}, \quad (8)$$

where $I = \text{diag}(I_{xx}, I_{yy}, I_{zz})$ is the inertia matrix around the axes of F_B . Direct computation of (8) leads to

$$\begin{pmatrix} I_{xx} \dot{p} \\ I_{yy} \dot{q} \\ I_{zz} \dot{r} \end{pmatrix} = \begin{pmatrix} \tau_\phi - (I_{zz} - I_{yy})qr \\ \tau_\theta - (I_{xx} - I_{zz})pr \\ \tau_\psi - (I_{yy} - I_{xx})pq \end{pmatrix}. \quad (9)$$

Summing up, Eq. (6), (7), and (9) are one possible nonlinear dynamic state space model of a quadrotor aircraft reads

$$\begin{aligned} \dot{x} &= u, \\ \dot{y} &= v, \\ \dot{z} &= w, \\ \dot{\phi} &= p c_\theta + r s_\theta, \\ \dot{\theta} &= \frac{s_\phi}{c_\phi} s_\theta p + q - \frac{s_\phi}{c_\phi} c_\theta r \\ \dot{\psi} &= -\frac{s_\theta}{c_\phi} p + \frac{c_\theta}{c_\phi} r, \\ \dot{u} &= (s_\theta c_\psi + s_\phi c_\theta s_\psi) \frac{F}{m} + \frac{W_x}{m}, \\ \dot{v} &= (s_\theta s_\psi - s_\phi c_\theta c_\psi) \frac{F}{m} + \frac{W_y}{m}, \end{aligned}$$

$$\begin{aligned} \dot{w} &= c_\phi c_\theta \frac{F}{m} - g + \frac{W_z}{m} \\ \dot{p} &= -\frac{I_{zz} - I_{yy}}{I_{xx}} q r + \frac{\tau_\phi}{I_{xx}}, \\ \dot{q} &= -\frac{I_{xx} - I_{zz}}{I_{yy}} p r + \frac{\tau_\theta}{I_{yy}}, \\ \dot{r} &= -\frac{I_{yy} - I_{zz}}{I_{zz}} p q + \frac{\tau_\psi}{I_{zz}}. \end{aligned} \quad (10)$$

III. DISTURBANCE NONLINEAR OBSERVER USING LIPSCHITZ METHOD

Consider a nonlinear model affected by unknown wind disturbance w as described as below

$$\begin{aligned} \dot{\xi}(t) &= A \xi(t) + f(\xi(t)) + g(u(t), \eta(t)) + D w(t), \\ \eta(t) &= C \xi(t), \end{aligned} \quad (11)$$

where $\xi \in \mathbb{R}^n$ is the state vector, $u \in \mathbb{R}^m$ is a known input vector, $w \in \mathbb{R}^k$ is the vector of the unknown input, $\eta \in \mathbb{R}^p$ is an output vector. Moreover, A is the state matrix, C is the output matrix, D is the disturbance matrix of suitable sizes, and $g : \mathbb{R}^{m+p} \rightarrow \mathbb{R}^n$ and $f : \mathbb{R}^n \rightarrow \mathbb{R}^n$ are nonlinear functions. Then, the nonlinear quadrotor model (10) in Sec. II can be written as in (11) by defining

$$A = \begin{pmatrix} 0_{3 \times 3} & I_{3 \times 3} & 0_{3 \times 3} & 0_{3 \times 3} \\ 0_{3 \times 3} & 0_{3 \times 3} & 0_{3 \times 3} & 0_{3 \times 3} \\ 0_{3 \times 3} & 0_{3 \times 3} & 0_{3 \times 3} & Q \\ 0_{3 \times 3} & 0_{3 \times 3} & 0_{3 \times 3} & 0_{3 \times 3} \end{pmatrix}, \text{ with } Q = \begin{pmatrix} 0 & 0 & 0 \\ 0 & 1 & 0 \\ 0 & 0 & 0 \end{pmatrix} \quad (12)$$

and

$$f(\xi) = \begin{pmatrix} 0_{5 \times 1} \\ -g \\ c_\theta p + s_\theta r \\ \frac{s_\phi}{c_\phi} s_\theta p + \frac{s_\phi}{c_\phi} c_\theta r \\ \frac{s_\theta}{c_\phi} p + \frac{c_\theta}{c_\phi} r \\ -\frac{I_{zz} - I_{yy}}{I_{xx}} q r \\ -\frac{I_{xx} - I_{zz}}{I_{yy}} p r \\ -\frac{I_{yy} - I_{xx}}{I_{zz}} p q \end{pmatrix}, \quad (13)$$

$$g(u, \eta) = \begin{pmatrix} 0_{3 \times 1} & 0_{3 \times 3} \\ \begin{pmatrix} s_\theta c_\psi + s_\phi c_\theta s_\psi \\ s_\theta c_\psi - s_\phi c_\theta c_\psi \\ c_\phi c_\theta \end{pmatrix} \frac{F}{m} & 0_{3 \times 3} \\ 0_{3 \times 1} & 0_{3 \times 3} \\ 0_{3 \times 1} & \Phi \end{pmatrix}, \quad (14)$$

where $\Phi = \text{diag}(\tau_\phi/I_{zz}, \tau_\theta/I_{yy}, \tau_\psi/I_{zz})$, and the unknown wind gust matrix is $D = (0_{3 \times 3}, 0_{3 \times 3}, I_{3 \times 3}/m, 0_{3 \times 3})^\top$.

The observer dynamics can be written as

$$\dot{\hat{\xi}} = A \hat{\xi} + f(\hat{\xi}) + g(u, \eta) + L(y - C\hat{x}). \quad (15)$$

For the system observer to in (11) and (15), the error dynamics $e = \xi - \hat{\xi}$ can be written as

$$\dot{e} = (A - LC)e + f(\xi) - f(\hat{\xi}), \quad (16)$$

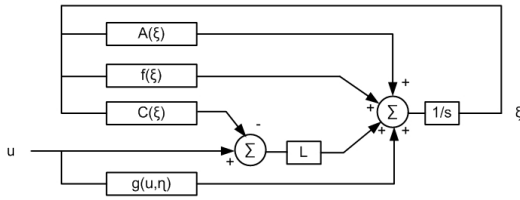


FIGURE 2. Lipschitz based unknown states observer structure.

where $f(\xi)$ is the nonlinearity present in the system that satisfies Lipschitz condition with a Lipschitz constant γ , that is,

$$|f(\xi) - f(\hat{\xi})| \leq \gamma \|\xi - \hat{\xi}\| \quad (17)$$

To address the nonlinearity (17) Let $f(\xi) : \mathbb{R}^n \rightarrow \mathbb{R}^n$ to be the nonlinear part of the dynamics such that $f(\xi) = [f_1(\xi), f_2(\xi), f_3(\xi), \dots, f_n(\xi)]$ where $f_i(\xi) : \mathbb{R}^n \rightarrow \mathbb{R}^n$. The term that will appear in state estimation error dynamics is $f(\xi) - f(\hat{\xi})$, and can be expressed as:

$$\begin{aligned} f(\xi) - f(\hat{\xi}) &= \begin{bmatrix} \frac{\partial f_1(\xi)}{\partial \xi_1(\xi)} & \dots & \frac{\partial f_1(\xi)}{\partial \xi_n(\xi)} \\ \vdots & \dots & \vdots \\ \frac{\partial f_n(\xi)}{\partial \xi_1(\xi)} & \dots & \frac{\partial f_n(\xi)}{\partial \xi_n(\xi)} \end{bmatrix} (\xi - \hat{\xi}) \\ &= \begin{bmatrix} h_{11} & \dots & h_{1n} \\ \vdots & \dots & \vdots \\ h_{n1} & \dots & h_{nn} \end{bmatrix} (\xi - \hat{\xi}) = \gamma e \quad (18) \end{aligned}$$

The Lipschitz constant of the vector-valued function $f(\xi)$ is $r = \sqrt{r_1^2 + r_2^2 + \dots + r_n^2}$, where r_i is the Lipschitz constant of $f_i(x) \forall i = 1 \dots n$ and can be expressed as $r_i = \sqrt{\gamma_1^2 + \gamma_2^2 + \dots + \gamma_n^2}$. The maximum and minimum values for positions and velocities of the Parrot Mambo Drone can be used to find γ for the quadrotor.

To show that the state estimation error dynamics is asymptotically stable, the Lyapunov candidate $V = e^T P e$, with $P > 0$, is used. Computing the derivative of V along the error trajectory gives

$$\dot{V} = \dot{e}^T P e + e^T P \dot{e}. \quad (19)$$

Substituting (16) into (19) the Lyapunov function then yields

$$\begin{aligned} \dot{V} &= e^T (A - LC)^T P + P(A - LC) e + \tilde{f}(x, \hat{x})^T P e \\ &\quad + e^T P \tilde{f}(x, \hat{x})^T, \quad (20) \end{aligned}$$

where $\tilde{f}(x, \hat{x}) = f(x) - f(\hat{x})$. As $\tilde{f}(x, \hat{x}) = f(x) - f(\hat{x})$ has a Lipschitz constant γ , then it holds

$$\|\tilde{f}(x, \hat{x})\|_2 \leq \gamma \|e\|_2. \quad (21)$$

Hence, substituting (21) into (20), yields

$$\begin{aligned} \dot{V} &= e^T [(A - LC)^T + P(A - LC)] e + \gamma \|e^T\| \|P e\|_2 \\ &\quad + \|e^T P\|_2 \gamma \|e\|_2. \quad (22) \end{aligned}$$

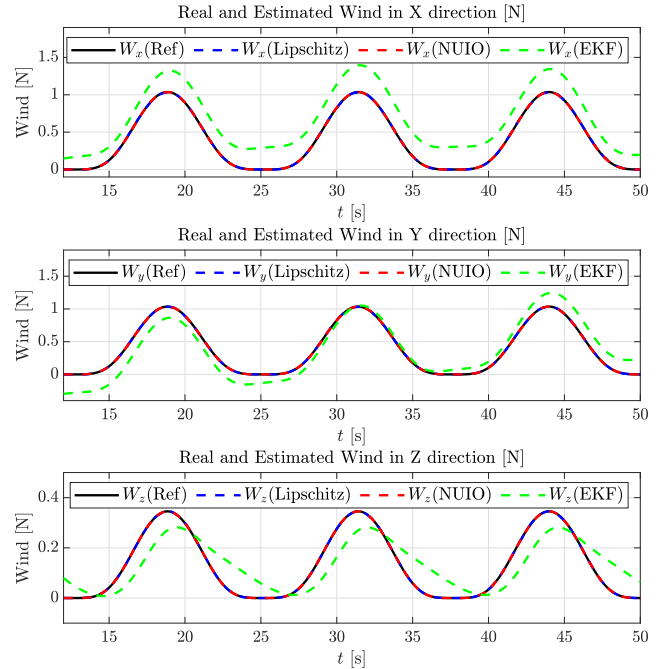


FIGURE 3. Estimated versus actual wind gusts for the time varying wind gust model.

By using the theorem $2ab = a^2 + b^2$, with $a = \gamma \|e\|$ and $b = \|e^T P\|$, hence, we have

$$\dot{V} = e^T [(A - LC)^T + P(A - LC)] e + \gamma^2 e e + e^T P P e \quad (23)$$

Finally, the derivative of the Lyapunov candidate is

$$\dot{V} = e^T [(A - LC)^T P + P(A - LC) + \gamma^2 I + P P] e. \quad (24)$$

Matrix P and the observer's gain matrix L are chosen so that the estimation error converges to zero, i.e. $e \rightarrow 0$ as $t \rightarrow \infty$ when

$$\begin{aligned} (A - LC)^T P + P(A - LC) + \gamma^2 I + P P < 0 \text{ and} \\ P > 0 \quad (25) \end{aligned}$$

Furthermore, (25) ensures the asymptotic stability of e if $V > 0$ and $\dot{V} < 0$. With $R = P L$, we obtain

$$A^T P + P A - C^T R - R C + \gamma I + P P < 0 \quad (26)$$

Using Schur complement lemma to convert to LMI so that it can be solved by Matlab, we take $R = -I$, $S = P$ and $Q = A^T P + P A - C^T R - R C + \gamma^2 I$. Hence, finally the LMI equations become

$$\begin{bmatrix} A^T P + P A - C^T R - R C + \gamma^2 I & P \\ P & P \end{bmatrix} < 0, \quad (27)$$

which can be solved for the decision matrix R , while the observer's gain matrix can be found as $L = P^{-1} R$ with P a symmetric and invertible matrix.

Moreover, the sought signal of the unknown input wind, W , can finally be computed after obtaining all states' estimates

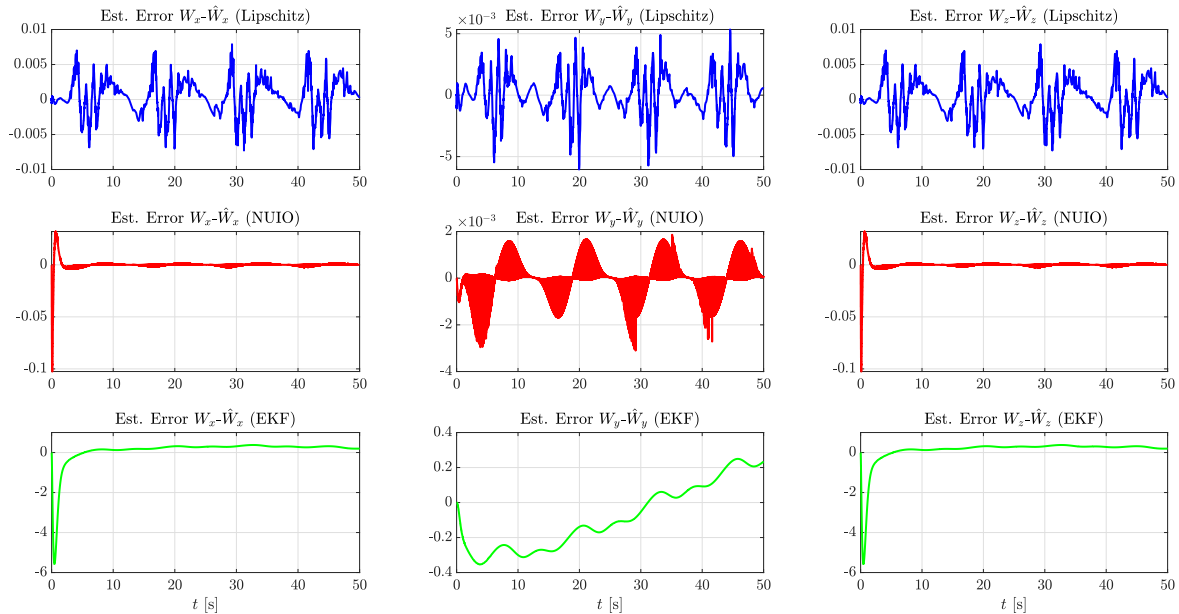


FIGURE 4. Error Estimated versus actual wind gusts for the time-varying wind as shown in Fig. 3 gust model for proposed method when compared to NUIO [5] and Extended Kalman Filter.

as

$$W = [D^T D]^{-1} D^T [\hat{\xi}(t) - A\hat{\xi}(t) - f(\hat{\xi}(t)) - g(u(t), \eta(t))]. \quad (28)$$

Fig. 6 illustrates the Lipschitz-based unknown input-state observer scheme.

Furthermore using the nonlinear dynamic model of the quadrotor mentioned in (12)-(14) used to model the behavior of a real quadrotor presented with external unknown wind disturbances and once all the states are observed, as given in Fig. 6, the proposed UIO reconstructs the unknown wind gust or unknown disturbance (W_x, W_y, W_z) acting on the quadrotor aircraft.

The effectiveness of the Lipschitz observer is significantly dependent on the choice of the Lipschitz constant, making the selection of an appropriate constant very important. An incorrect choice in this regard can result in poor observer performance. Moreover, Lipschitz observers rely on mathematical models of the system, and any inaccuracies or discrepancies in these models can negatively impact the observer’s performance, compromising its accuracy and effectiveness.

Extended Kalman Filters (EKF) and Nonlinear unknown input-state observer (NUIO) [5] is compared to the proposed Lipschitz-based unknown input-state observer. Fig 3 shows the estimation of time-varying wind gusts by the three observers mentioned before. This is chosen as time varying wind gust is more complicated to estimate than the step wind gusts. It can be easily noted that the Lipschitz-based observer and NUIO have superior performance than the EKF. In addition, different process noise and measurement noise values were simulated for the EKF, from which the optimal process noise and measurement noise values were selected.

Moreover, the difference between Lipschitz-based observer and EKF can only be compared in Fig. 4 which shows that the proposed Lipschitz error is 10 times smaller than the one of NUIO.

IV. COMPENSATION OF THE WIND DISTURBANCE

The Lipschitz UIO estimates the unknown wind gusts in real-time, as described in the previous section, and provides this information to a PD controller in order to compensate for it and regulate the quadrotor’s nonlinear model. Having denoted with (x_d, y_d, z_d, psi_d) the desired aircraft’s pose, an Attitude Control is used for the orientation in ϕ, θ, ψ , while a Position Control is used for positioning the quadrotor along the axes x, y , and z , by employing the estimated wind gusts $\hat{W}_x, \hat{W}_y, \hat{W}_z$. According to the obtained results, the quadrotor is in a hovering state, which implies that $\phi, \theta \approx 0$ for the system to be fully controllable, which consists of 4 inputs and 4 outputs. $x, y, z, \phi, \theta, \psi, u, v, w$ are the nine simulation-measurable states fed to the proposed observer, out of a total of 12. The Lipschitz UIO uses these to estimate the three remaining states as well as the three unknown wind gust components.

A simple yet effective PD control algorithm has been developed in Matlab/Simulink with the proposed observer. The Parrot Mambo quadrotor has been used to test the results in simulation and experiments. The wind gusts vectors $(W_x, W_y, W_z)^T$ affecting the aircraft’s position is compensated by the PD controller by varying the four rotor speeds. The PD controller is based on the approximated linear dynamic model of the quadrotor aircraft in hovering condition when $\phi, \theta \approx 0$. Let such nominal conditions be described by (x_d, y_d, z_d, ψ_d) and the nominal force for hovering, $\bar{f} = g$. Hence, the tracking error variables be $\delta x = x - x_d$,

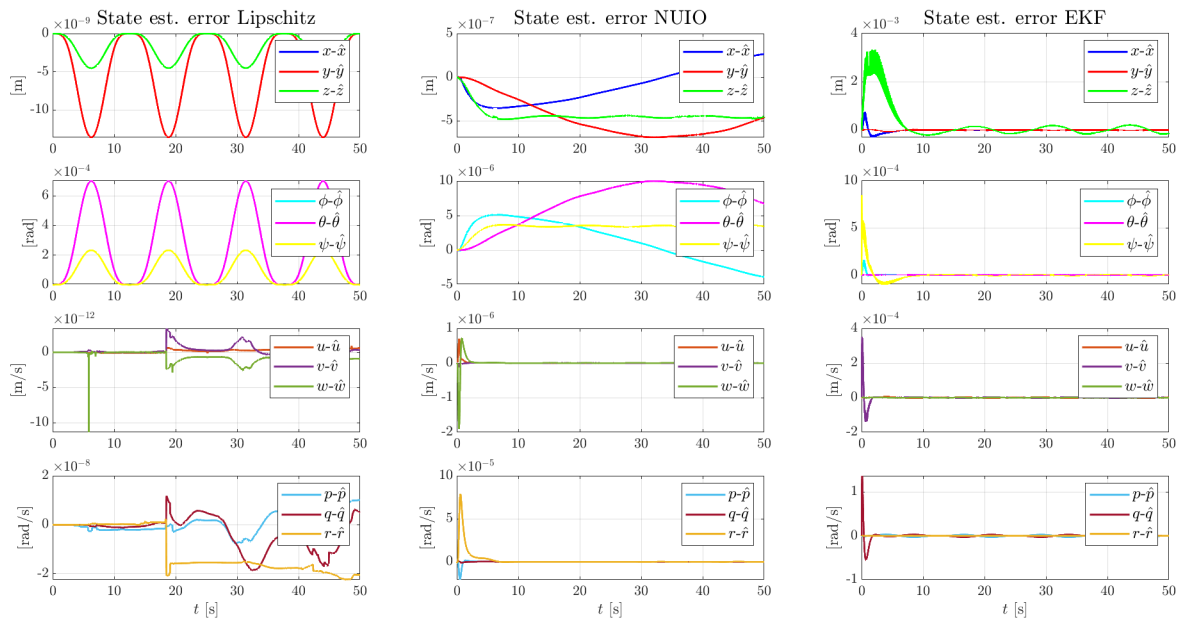


FIGURE 5. Plots of state estimation errors of the proposed Lipschitz (left) vs an NUIO (middle) and a EKF (right).

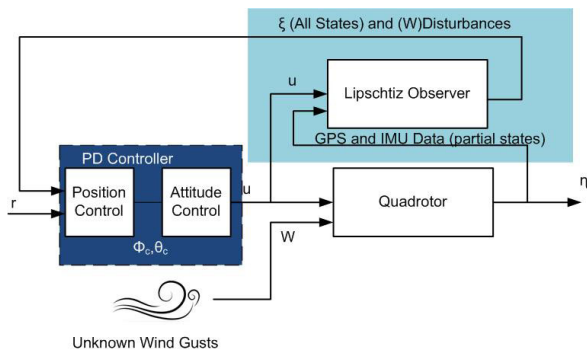


FIGURE 6. Proposed system architecture, the aircraft pose information within the observer provides accurate information to the controller for precise position.

$\delta y = y - y_d$, $\delta z = z - z_d$, and $\delta \psi = \psi - \psi_d$. Moreover, the input variation variables are $\delta f = f - g$, $\delta \phi = \phi - \phi_C$, and $\delta \theta = \theta - \theta_C$. The linearized model of the linear position is

$$\begin{pmatrix} \ddot{x} \\ \ddot{y} \\ \ddot{z} \end{pmatrix} = \begin{pmatrix} (gs_{\psi_d} \delta \phi + gc_{\psi_d} \delta \theta)/m + \frac{W_x}{m} \\ -(gs_{\psi_d} \delta \phi + gs_{\psi_d} \delta \theta)/m + \frac{W_y}{m} \\ \frac{(\delta f + W_z)}{m} \end{pmatrix} \quad (29)$$

where $\delta f \approx \frac{8K_F \omega_0}{m} (\delta \omega_1 + \delta \omega_2 + \delta \omega_3 + \delta \omega_4)$. To ensure the asymptotic convergence of the quadrotor center of mass to the desired position, the dynamic model in (29) is forced to follow the dynamics

$$\begin{pmatrix} \ddot{x} \\ \ddot{y} \\ \ddot{z} \end{pmatrix} = - \begin{pmatrix} k_x^v \dot{x} + k_x^p \delta x \\ k_y^v \dot{y} + k_y^p \delta y \\ k_z^v \dot{z} + k_z^p \delta z \end{pmatrix}. \quad (30)$$

By comparing (29) and (30), the relations for the rotor speed variations and the commanded roll and pitch,

ϕ_C and θ_C are obtained as follows:

$$\begin{pmatrix} \phi_C \\ \theta_C \\ f \end{pmatrix} = \begin{pmatrix} -\frac{R(\psi_d)}{g} \left(k_x^v \dot{x} + k_x^p (x - x_d) - \frac{W_x}{m} \right) \\ -\frac{R(\psi_d)}{g} \left(k_y^v \dot{y} + k_y^p (y - y_d) - \frac{W_y}{m} \right) \\ \frac{K_F}{m} \sum_{i=1}^4 \omega_i^2 + 2\sqrt{\frac{K_F}{m}} \delta \omega_z + \frac{W_z}{m} \end{pmatrix} \quad (31)$$

where

$$R(\psi_d) = \begin{pmatrix} s_{\psi_d} & -c_{\psi_d} \\ c_{\psi_d} & s_{\psi_d} \end{pmatrix},$$

$$\delta \omega_z = -k_z^v \dot{z} - k_z^p (x - z_d) + \frac{W_z}{m}.$$

Moving now on to the angular velocity, from the torque's equations (2), the angular accelerations (9) and using the hovering condition which is $\phi, \theta \approx 0$, thus it equates that $\dot{\phi} \approx p$, $\dot{\theta} \approx q$, and $\dot{\psi} \approx r$ (from 10). The attitude dynamics simplifies to

$$\begin{pmatrix} \ddot{\phi} \\ \ddot{\theta} \\ \ddot{\psi} \end{pmatrix} = \begin{pmatrix} \frac{IK_F}{I_{xx}} (\omega_2^2 - \omega_4^2) - \frac{I_{zz} - I_{yy}}{I_{xx}} \dot{\theta} \dot{\psi} \\ \frac{IK_F}{I_{yy}} (\omega_3^2 - \omega_1^2) - \frac{I_{xx} - I_{zz}}{I_{yy}} \dot{\phi} \dot{\psi} \\ \frac{K_M}{I_{zz}} (\omega_1^2 - \omega_2^2 + \omega_3^2 - \omega_4^2) - \frac{I_{xx} - I_{yy}}{I_{zz}} \dot{\phi} \dot{\theta} \end{pmatrix}. \quad (32)$$

The quantitative analysis of results using Integral Time Absolute Error (ITAE) from Fig. 5 is computed to show the performance of the proposed controller with respect to the NUIO and EKF is presented in Table 1.

After linearizing (32) around the hovering condition with $\omega_i \approx \omega_0 = \sqrt{\frac{mg}{4K_F}}$. Having denoted $\delta \psi = \psi - \psi_d$ and $\delta \omega_i = \omega_i - \omega_0$, the linearized model reads

$$\begin{pmatrix} \ddot{\phi} \\ \ddot{\theta} \\ \delta \ddot{\psi} \end{pmatrix} = \begin{pmatrix} \frac{l\sqrt{mgK_F}}{I_{xx}} (\delta \omega_2^2 - \delta \omega_4^2) \\ \frac{l\sqrt{mgK_F}}{I_{yy}} (\delta \omega_3^2 - \delta \omega_1^2) \\ \frac{K_M \sqrt{mgK_F}}{I_{zz}} (\delta \omega_1^2 - \delta \omega_2^2 + \delta \omega_3^2 - \delta \omega_4^2) \end{pmatrix} \quad (33)$$

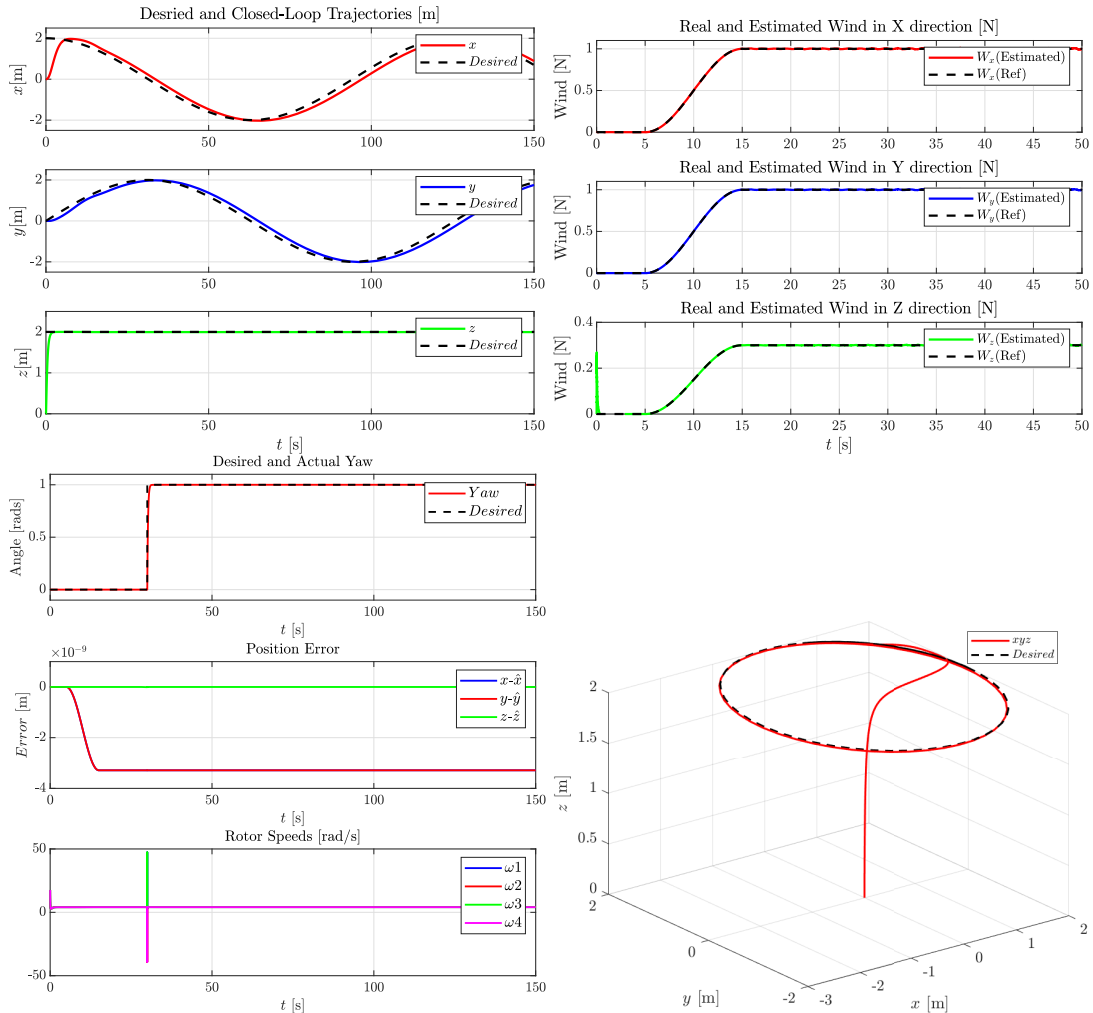


FIGURE 7. Simulation results of wind estimation of Parrot Mambo for time-varying wind gusts and desired and closed-loop spiral trajectories in 3D space.

TABLE 1. ITAE error comparison of Lipschitz vs NUIO vs EKF.

ξ	Lipschitz	NUIO	EKF
x	6.7×10^{-6}	2.0×10^{-4}	7.9×10^{-3}
y	6.7×10^{-6}	7.1×10^{-4}	6.3×10^{-3}
z	2.2×10^{-6}	5.7×10^{-4}	1.6×10^{-1}
ϕ	3.4×10^{-1}	2.9×10^{-3}	4.0×10^{-4}
θ	3.4×10^{-1}	1.0×10^{-3}	3.0×10^{-4}
ψ	1.1×10^{-1}	4.3×10^{-3}	8.1×10^{-3}
u	4.2×10^{-10}	2.2×10^{-7}	3.6×10^{-3}
v	7.0×10^{-10}	8.4×10^{-7}	3.6×10^{-3}
w	1.2×10^{-9}	1.3×10^{-6}	1.0×10^{-5}
p	4.7×10^{-6}	1.5×10^{-5}	1.7
q	8.5×10^{-6}	3.0×10^{-5}	1.7
r	1.9×10^{-5}	1.8×10^{-4}	7.5×10^{-1}

Equating the aircraft’s orientation to the PD controller variables, where all constants are based on desired eigenvalues locations, $\delta\phi = \phi - \phi_C$ and $\delta\theta = \theta - \theta_C$, where ϕ_C and θ_C are commanded roll and pitch values fed to attitude controller

$$\begin{pmatrix} \delta\omega_2 - \delta\omega_4 \\ \delta\omega_3 - \delta\omega_1 \\ \delta\omega_1 - \delta\omega_2 + \delta\omega_3 - \delta\omega_4 \end{pmatrix} = \begin{pmatrix} -k_\phi^v \dot{\phi} - k_\phi^p \phi \\ -k_\theta^v \dot{\theta} - k_\theta^p \theta \\ -k_\psi^v \dot{\psi} - k_\psi^p \psi \end{pmatrix}$$

Considering the cross configuration of the quadrotor aircraft and equating it to find the variable speed of each rotor gives

$$\begin{pmatrix} \delta\omega_1 \\ \delta\omega_2 \\ \delta\omega_3 \\ \delta\omega_4 \end{pmatrix} = \frac{1}{4} \begin{pmatrix} 1 & 0 & -2 & 1 \\ 1 & 2 & 0 & -1 \\ 1 & 0 & 2 & 1 \\ 1 & -2 & 0 & -1 \end{pmatrix} \begin{pmatrix} \delta\omega_z \\ \delta\omega_\phi \\ \delta\omega_\theta \\ \delta\omega_\psi \end{pmatrix}$$

Note in practical each $\delta\omega_i$ is added to corresponding hovering speed. Finally the equation of the rotor speed, compensating the wind gusts, is

$$\begin{pmatrix} \omega_1 \\ \omega_2 \\ \omega_3 \\ \omega_4 \end{pmatrix} = \frac{\begin{pmatrix} \frac{1}{4} & 0 & \frac{I_{yy}}{2I} & -\frac{I_{zz}}{KM} \\ \frac{1}{4} & -\frac{I_{xx}}{2I} & 0 & \frac{I_{zz}}{KM} \\ \frac{1}{4} & 0 & \frac{I_{yy}}{2I} & -\frac{I_{zz}}{KM} \\ \frac{1}{4} & \frac{I_{xx}}{2I} & 0 & \frac{I_{zz}}{KM} \end{pmatrix}}{\sqrt{mgK_F}} \begin{pmatrix} 2mg + \sqrt{mgK_F}\delta\omega_z \\ k_\phi^v \dot{\phi} + k_\phi^p(\phi - \phi_C) \\ k_\theta^v \dot{\theta} + k_\theta^p(\theta - \theta_C) \\ k_\psi^v \dot{\psi} + k_\psi^p(\psi - \psi_d) \end{pmatrix} \quad (34)$$

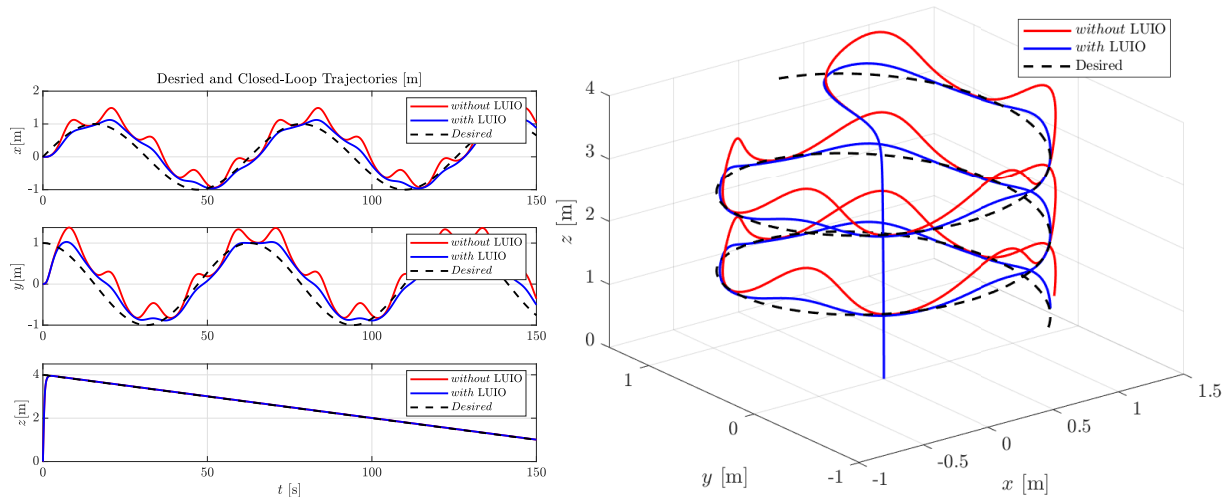


FIGURE 8. Results of wind estimation of Parrot Mambo for horizontal time varying wind gusts and desired and closed-loop spiral trajectories in 3D space for with and without disturbance observer.

TABLE 2. Parrot minidrone hardware parameters.

Parameter	Value	Unit	Symbol
Weight	6.95×10^{-2}	kg	m
Arm Length	6.20×10^{-2}	m	l
Inertial moment about x	6.86×10^{-5}	kg m ²	I_x
Inertial moment about y	9.20×10^{-5}	kg m ²	I_y
Inertial moment about z	1.36×10^{-4}	kg m ²	I_z
Motor Thrust Factor	1.00×10^{-2}	N rad ⁻² s ⁻²	k_f
Motor Torque Factor	7.82×10^{-4}	N m rad ⁻² s ⁻²	k_m
Gravitational Acceleration	9.98	m s ⁻²	g

V. RESULTS AND DISCUSSION

The Parrot Rolling Spider minidrone was used together with a base station containing a laptop computer with Matlab/Simulink installed. The Parrot Rolling Spider is a programmable indoor minidrone. Its sensors include a 3-axis gyroscope for attitude sensing, a 3-axis accelerometer, a camera for visual navigation to detect x-y position, and ultrasonic sensors with a pressure sensor that estimates flight altitude. The parameters of the parrot drone are presented in Table 2.

A. SIMULATION RESULTS

The proposed scheme has first been validated in Matlab/Simulink with the parameters of the nonlinear quadrotor model, where its parameters are in Table 2. The purpose of this step is to show the main behavior of the proposed method under ideal conditions with the presence of external disturbances, which in this case are wind gusts. However, other uncertainties such as model uncertainties, delays due to propeller dynamics and noise have not been taken into account in the simulation. The Lipschitz UIO is simulated in continuous time. The control system has been tested while the quadrotor is required to perform a complicated task: maintaining a circular trajectory in the presence of x, y and z wind gusts as a ramp input.

Fig. 7 shows the effectiveness of the proposed estimation and control methods. As the Lipschitz UIO reconstructs

the wind force component and provides the signal values to the controller for compensation, the quadrotor quickly reaches the desired position. The controller commands the rotor speeds via a signal ensuring that the quadrotor receives the correct thrust force, leading to appropriate roll and pitch angles. The rotor speed plot in Fig. 7 shows how the controller compensates for the wind gust force by varying the rotor speeds. This shows that the controller can easily compensate for the effect of wind gusts to maintain the precise position of the quadrotor. The position error, shown in Fig. 7, is very small and can be neglected.

B. HARDWARE RESULTS

The final step is to validate the proposed scheme in experiments on a real parrot rolling spider minidrone. The parrot rolling spider is used together with a base station that has a laptop with Matlab Simulink installed. The parrot rolling spider is a programmable indoor minidrone where the flight control system can be edited to the proposed scheme. The drone has a 3-axis gyroscope for attitude measurement, a 3-axis accelerometer, a camera for visual navigation to sense the x-y position, and ultrasonic sensors with a pressure sensor that work together to estimate its flying altitude. The hardware support package for the Parrot Minidrone is available for Matlab. This enables testing and verification to be done in Matlab Simulink on the minidrone. The parameters for the parrot mambo are the same as in Table 2.

A Bluetooth personal area network (PAN) is used to connect the minidrone to the workstation laptop for programming. After completing the controller design, the Flight Controller Subsystem in Simulink is converted into C code and uploaded onto the minidrone through the Bluetooth PAN. Upon uploading the code, a command is given from Simulink to initiate the experiment. The connection between the minidrone and the Simulink environment is in real-time. After a flight experiment, the experimental flight data, including the positions, velocities, and rotor speeds, are

TABLE 3. The range of positions and velocities for Parrot minidrone to calculate γ .

Positions	Range	Velocities	Range
x	0, 20m	u	0, 2m/s
y	0, 20m	v	0, 2m/s
z	0, 20m	w	0, 2m/s
ϕ	$-\pi, \pi$ rad	p	0, 0.3rad/s
θ	$-\pi, \pi$ rad	q	0, 0.3rad/s
ψ	$-\frac{\pi}{2}, \frac{\pi}{2}$ rad	r	0, 0.3rad/s

transferred from the minidrone to the Matlab workspace via the Bluetooth PAN. Post-flight analysis is then done with the data recorded into the Matlab workspace.

The quadrotor receives the desired positions (x_d, y_d, z_d, ψ_d) and the IMU with position sensors measures partial states which are $x, y, z, \phi, \theta, \psi, u, v, w$. The partial states and the rotor speeds are then given to the Lipschitz NUIO to reconstruct all 12 states and estimate the wind gusts. Moreover, this information is then fed back to the PD controller of the parrot Mambo. As it is very difficult to provide and measure time-varying wind in a real-world scenario, the horizontal step wind of $W_x = 1N, W_y = 1N$ is exposed to the quadrotor from 0s.

According to parrot mini drone, the maximum and minimum values of positions and velocities to calculate the lipschtiz constant γ is shown in Table 3.

Fig. 8 depicts the hardware results for time-varying wind gusts, allowing the proposed concept to be rigorously examined. The quadrotor is given a spiral trajectory and is exposed to time-varying (as depicted in Fig. 3) horizontal wind from the x and y. With a slight delay, the quadrotor can be seen to be very close to the reference. This can be caused by bandwidth delays in actuators. Moreover, in Fig. 8, we present the performance of the flight with the disturbance observer, while also including the system without the disturbance observer for comparison. The results unmistakably illustrate that the graph corresponding to the proposed system produces superior outcomes in our experiments.

VI. CONCLUSION

In conclusion, this paper presents an alternative and effective method to accurately estimate and compensate for external disturbances, such as wind gusts, acting on the nonlinear quadrotor aircraft model in real time. Matlab/Simulink and experiments validate the robust performance of the quadrotor, which moves accurately along the desired path when exposed to different types of wind gusts. This demonstrates that the proposed method does not require additional sensors, is computationally simple, and can provide rapid response to various types of flight disturbances. In addition, the Lipschitz incognito input observer is compatible with any type of controller, as long as the latter can adjust the aircraft rotor speed to compensate for the estimated wind gusts. To make the system adaptive, future work will focus on online parameter estimation and adaptation algorithms to enhance the controller's performance. Another future work can be the coordination and cooperation of multiple UAV quadrotors operating in windy conditions. The strategies would be

distributed control, communication, and decision-making using observers for efficient navigation and task execution in the presence of wind disturbances. Also, in future real-world validation and testing can be carried out to test the effectiveness of the method such as using UAV for agricultural imagery in different terrains with wind patterns. Since this method uses minimum sensors, the energy-aware algorithms and can be incorporated to test the energy efficiency. Finally, this independent and robust control method has multiple real-world applications, such as piloting a quadcopter independently and accurately in windy conditions.

REFERENCES

- [1] H. Shakhatreh, A. H. Sawalmeh, A. Al-Fuqaha, Z. Dou, E. Almaita, I. Khalil, N. S. Othman, A. Khreishah, and M. Guizani, "Unmanned aerial vehicles (UAVs): A survey on civil applications and key research challenges," *IEEE Access*, vol. 7, pp. 48572–48634, 2019.
- [2] L. Chen, Z. Liu, Q. Dang, W. Zhao, and G. Wang, "Robust trajectory tracking control for a quadrotor using recursive sliding mode control and nonlinear extended state observer," *Aerosp. Sci. Technol.*, vol. 128, Sep. 2022, Art. no. 107749. [Online]. Available: <https://www.sciencedirect.com/science/article/pii/S1270963822004230>
- [3] Y. Lei, Y. Huang, and H. Wang, "Effects of wind disturbance on the aerodynamic performance of a quadrotor MAV during hovering," *J. Sensors*, vol. 2021, pp. 1–13, Apr. 2021.
- [4] S. I. Azid, K. Kumar, M. Cirrincione, and A. Fagiolini, "Wind gust estimation for precise quasi-hovering control of quadrotor aircraft," *Control Eng. Pract.*, vol. 116, Nov. 2021, Art. no. 104930. [Online]. Available: <https://www.sciencedirect.com/science/article/pii/S0967066121002070>
- [5] S. I. Azid, K. Kumar, M. Cirrincione, and A. Fagiolini, "Robust motion control of nonlinear quadrotor model with wind disturbance observer," *IEEE Access*, vol. 9, pp. 149164–149175, 2021.
- [6] J. L. Guzmán and T. Häggglund, "Simple tuning rules for feedforward compensators," *J. Process Control*, vol. 21, no. 1, pp. 92–102, Jan. 2011. [Online]. Available: <https://www.sciencedirect.com/science/article/pii/S0959152410001939>
- [7] J.-Y. Wang, B. Luo, M. Zeng, and Q.-H. Meng, "A wind estimation method with an unmanned rotorcraft for environmental monitoring tasks," *Sensors*, vol. 18, no. 12, p. 4504, Dec. 2018.
- [8] S. I. Abdelmaksoud, M. Mailah, and A. M. Abdallah, "Robust intelligent self-tuning active force control of a quadrotor with improved body jerk performance," *IEEE Access*, vol. 8, pp. 150037–150050, 2020.
- [9] D. J. Almkhles, "Robust backstepping sliding mode control for a quadrotor trajectory tracking application," *IEEE Access*, vol. 8, pp. 5515–5525, 2020.
- [10] H. Liu, W. Zhao, S. Hong, F. L. Lewis, and Y. Yu, "Robust backstepping-based trajectory tracking control for quadrotors with time delays," *IET Control Theory Appl.*, vol. 13, no. 12, pp. 1945–1954, Aug. 2019, doi: [10.1049/iet-cta.2018.6043](https://doi.org/10.1049/iet-cta.2018.6043).
- [11] L. Liu, S. Ding, and X. Yu, "Second-order sliding mode control design subject to an asymmetric output constraint," *IEEE Trans. Circuits Syst. II, Exp. Briefs*, vol. 68, no. 4, pp. 1278–1282, Apr. 2021.
- [12] G. Wang, "Adaptive sliding mode robust control based on multi-dimensional Taylor network for trajectory tracking of quadrotor UAV," *IET Control Theory Appl.*, vol. 14, no. 14, pp. 1855–1866, Sep. 2020, doi: [10.1049/iet-cta.2019.1058](https://doi.org/10.1049/iet-cta.2019.1058).
- [13] O. Mofid, S. Mobayen, and A. Fekih, "Adaptive integral-type terminal sliding mode control for unmanned aerial vehicle under model uncertainties and external disturbances," *IEEE Access*, vol. 9, pp. 53255–53265, 2021.
- [14] H. Liu, X. Wang, and Y. Zhong, "Robust position control of a lab helicopter under wind disturbances," *IET Control Theory Appl.*, vol. 8, no. 15, pp. 1555–1565, Oct. 2014, doi: [10.1049/iet-cta.2013.0799](https://doi.org/10.1049/iet-cta.2013.0799).
- [15] V. P. Shankaran, S. I. Azid, U. Mehta, and A. Fagiolini, "Improved performance in quadrotor trajectory tracking using MIMO PI²-D control," *IEEE Access*, vol. 10, pp. 110646–110660, 2022.
- [16] R. Kumar, S. Agarwal, and M. Kumar, "Modeling and control of a tethered tilt-rotor quadcopter with atmospheric wind model," *IFAC-PapersOnLine*, vol. 54, no. 20, pp. 463–468, 2021.

- [17] W.-H. Chen, J. Yang, L. Guo, and S. Li, "Disturbance-observer-based control and related methods—An overview," *IEEE Trans. Ind. Electron.*, vol. 63, no. 2, pp. 1083–1095, Feb. 2016.
- [18] D. D. Dhadekar and S. E. Talole, "Modified GESO based control for systems with sinusoidal disturbances," *IFAC-PapersOnLine*, vol. 53, no. 1, pp. 19–26, 2020. [Online]. Available: <https://www.sciencedirect.com/science/article/pii/S2405896320300215>
- [19] C. Hajiyeve, S. Y. Vural, A. Shumsky, and A. Zhirabok, "Robust Kalman filter based estimation of AUV dynamics in the presence of sensor faults," *IFAC-PapersOnLine*, vol. 51, no. 30, pp. 424–429, 2018. [Online]. Available: <https://www.sciencedirect.com/science/article/pii/S2405896318330003>
- [20] C. Hajiyeve and H. E. Soken, "Robust adaptive Kalman filter for estimation of UAV dynamics in the presence of sensor/actuator faults," *Aerosp. Sci. Technol.*, vol. 28, no. 1, pp. 376–383, Jul. 2013.
- [21] H. Wang, V. Ghaffari, S. Mobayen, A. Bartoszewicz, A. Fekih, and W. Assawinchaichote, "Finite-time robust performance improvement for non-linear systems in the presence of input non-linearity and external disturbance," *IET Control Theory Appl.*, vol. 17, no. 6, pp. 672–682, 2023, doi: [10.1049/cth2.12387](https://doi.org/10.1049/cth2.12387).
- [22] X. Lyu, J. Zhou, H. Gu, Z. Li, S. Shen, and F. Zhang, "Disturbance observer based hovering control of quadrotor tail-sitter VTOL UAVs using H_∞ synthesis," *IEEE Robot. Autom. Lett.*, vol. 3, no. 4, pp. 2910–2917, Oct. 2018.
- [23] A. Asignacion, S. Suzuki, R. Noda, T. Nakata, and H. Liu, "Frequency-based wind gust estimation for quadrotors using a nonlinear disturbance observer," *IEEE Robot. Autom. Lett.*, vol. 7, no. 4, pp. 9224–9231, Oct. 2022.
- [24] D. Caporale, A. Settini, F. Massa, F. Amerotti, A. Corti, A. Fagiolini, M. Guiggiani, A. Bicchi, and L. Pallottino, "Towards the design of robotic drivers for full-scale self-driving racing cars," in *Proc. Int. Conf. Robot. Autom. (ICRA)*, May 2019, pp. 5643–5649.
- [25] B. Zhu, M. Chen, and T. Li, "State prediction based control schemes for nonlinear systems with input delay and external disturbance," *IET Control Theory Appl.*, vol. 15, no. 13, pp. 1697–1707, Sep. 2021, doi: [10.1049/cth2.12152](https://doi.org/10.1049/cth2.12152).
- [26] G. Hattenberger, M. Bronz, and J.-P. Condomines, "Estimating wind using a quadrotor," *Int. J. Micro Air Vehicles*, vol. 14, Jan. 2022, Art. no. 175682932110708, doi: [10.1177/17568293211070824](https://doi.org/10.1177/17568293211070824).
- [27] D. Hentzen, T. Stastny, R. Siegwart, and R. Brockers, "Disturbance estimation and rejection for high-precision multirotor position control," in *Proc. IEEE/RSJ Int. Conf. Intell. Robots Syst. (IROS)*, Nov. 2019, pp. 2797–2804.
- [28] J. Jia, K. Guo, X. Yu, W. Zhao, and L. Guo, "Accurate high-maneuvering trajectory tracking for quadrotors: A drag utilization method," *IEEE Robot. Autom. Lett.*, vol. 7, no. 3, pp. 6966–6973, Jul. 2022.
- [29] E. Sariyildiz, R. Mutlu, and C. Zhang, "Active disturbance rejection based robust trajectory tracking controller design in state space," *J. Dyn. Syst., Meas., Control*, vol. 141, no. 6, Jun. 2019.
- [30] E. Sariyildiz, R. Oboe, and K. Ohnishi, "Disturbance observer-based robust control and its applications: 35th anniversary overview," *IEEE Trans. Ind. Electron.*, vol. 67, no. 3, pp. 2042–2053, Mar. 2020.



SOHAIL AHMAD ALI (Graduate Student Member, IEEE) received the bachelor's degree in electrical and electronics engineering from The University of the South Pacific, in 2022. He is currently pursuing the M.Sc. degree in engineering (research) focusing on the control of power electronics systems, the integration of renewable energy resources, and the application of grid-forming inverters to weak grids. He received the Gold Medal from The University of the South Pacific, for his academic achievements.



MESHACH KUMAR received the bachelor's degree in electrical and electronics engineering from The University of the South Pacific (USP), Fiji, where he is currently pursuing the master's degree with the School of Information Technology, Engineering, Mathematics and Physics. His research interests include fractional order control, system identification, and machine learning.



MAURIZIO CIRRINCIONE (Senior Member, IEEE) was born in May 1961. He received the Laurea degree from Politecnico di Torino, Turin, Italy, in 1991, and the Ph.D. degree from the University of Palermo, Italy, in 1996, both in electrical engineering. From 1996 to 2005, he was a Researcher with the ISSIA-CNR (Institute on Intelligent Systems for Automation), Palermo. Since 2005, he has been a Full Professor of control systems with UTBM, Belfort, France; and a member of the IRTES Laboratory and the Fuel Cell Laboratory (FCLab), Belfort, where he has been a first class Full Professor, since 2016. Since April 2014, he has been the Head of the School of Engineering and Physics, The University of the South Pacific, Suva, Fiji. He is the author of over 155 papers, 55 of which on high impact factor journals and two books. He received the 1997 "E. R. Caianiello" Prize in 1997 for the Best Italian Ph.D. Thesis on Neural Networks.



ADRIANO FAGIOLINI (Member, IEEE) received the M.S. degree in computer science engineering and the Ph.D. degree in robotics and automation from the University of Pisa, in 2004 and 2009, respectively. He is an Assistant Professor with the University of Palermo, Italy. He was a Visiting Researcher with the Department of Energy, IUT Longwy, Université de Lorraine, France, in 2019; and the Department of Mechanical Engineering, University of California at Riverside, from 2015 to 2017. He has enrolled with the Summer Student Program, European Center for Nuclear Research (CERN), Geneva, in 2002. In 2008, he led the team of the University of Pisa, during the first European Space Agency's Lunar Robotics Challenge, which resulted in a second-place prize for the team. He was one of the recipients of the IEEE ICRA Best Manipulation Paper Award, in 2005.



SHEIKH IZZAL AZID (Member, IEEE) received the M.Sc. degree in engineering in the area of automation and intelligent systems, in 2010, and the Ph.D. degree in aerial robotics and robust control from The University of the South Pacific in collaboration with the University of Palermo, Italy. He is a lecturer of engineering. He was as a consultant for several European projects on science, technology, and innovation in the Pacific. He was a recipient of the Erasmus+ Staff Exchange Program and he was attached with the Technical University of Sofia and the University of Palermo. His research interests include robotics, robust controls, autonomous systems, state observers, and unmanned aerial vehicles. He is the Vice President of IEEE VTS New Zealand North. He was a recipient of the IEEE Young Humanitarian Award.